

Optimal Active Control of Vehicle Suspension System Including Time Delay and Preview for Rough Roads

Javad Marzbanrad, Goodarz Ahmadi, Yousef Hojjat and Hassan Zohoor

Journal of Vibration and Control 2002 8: 967

DOI: 10.1177/107754602029586

The online version of this article can be found at:

<http://jvc.sagepub.com/content/8/7/967>

Published by:



<http://www.sagepublications.com>

Additional services and information for *Journal of Vibration and Control* can be found at:

Email Alerts: <http://jvc.sagepub.com/cgi/alerts>

Subscriptions: <http://jvc.sagepub.com/subscriptions>

Reprints: <http://www.sagepub.com/journalsReprints.nav>

Permissions: <http://www.sagepub.com/journalsPermissions.nav>

Citations: <http://jvc.sagepub.com/content/8/7/967.refs.html>

>> [Version of Record](#) - Oct 1, 2002

[What is This?](#)

Optimal Active Control of Vehicle Suspension System Including Time Delay and Preview for Rough Roads

JAVAD MARZBANRAD

Department of Mechanical and Aeronautical Engineering, Clarkson University, Potsdam, NY 13699-5725, USA, marzbanj@clarkson.edu, Department of Vehicle, Iran Science and Technology, Tehran, I.R. Iran

GOODARZ AHMADI

Department of Mechanical and Aeronautical Engineering, Clarkson University, Potsdam, NY 13699-5725, USA, ahmadi@clarkson.edu

YOUSEF HOJJAT

Department of Mechanical Engineering, Tarbiat Modarres University, Tehran, I.R. Iran

HASSAN ZOHOOR

Department of Mechanical Engineering, Sharif University of Technology, Tehran, I.R. Iran

(Received 2 March 2001; accepted 26 April 2002)

Abstract: An optimal preview control of a vehicle suspension system traveling on a rough road is studied. A three-dimensional seven degree-of-freedom car-riding model and several descriptions of the road surface roughness heights, including haversine (hole/bump) and stochastic filtered white noise models, are used in the analysis. It is assumed that contact-less sensors affixed to the vehicle front bumper measure the road surface height at some distances in the front of the car. The suspension systems are optimized with respect to ride comfort and road holding preferences including accelerations of the sprung mass, tire deflection, suspension rattle space and control force. The performance and power demand of active, active and delay, active and preview systems are evaluated and are compared with those for the passive system. The results show that the optimal preview control improves all aspects of the vehicle suspension performance while requiring less power. Effects of variation of preview time and variations in the road condition are also examined.

Key Words: Optimal control, active suspension, preview control, Random road.

1. INTRODUCTION

Developing advanced active suspension systems have has attracted considerable attention in modern vehicle system designs in recent years. The purpose of the suspension is to attenuate the vehicle vibrations due to various road excitations. The suspension system must also support the vehicle body, provide comfort for the riders, retain the vehicle stability during various handling actions, control body and wheel attitude, and minimize the vertical force

variation of the road-to-tire contact. Ride comfort is related to reducing the acceleration of sprung mass that requires small suspension forces, while good road holding, which assures more stability needs large dynamic suspension forces.

Ride comfort is related to reducing the acceleration of sprung mass. This normally requires small suspension forces. Good road holding, which assures stability, is related to lower acceleration of unsprung masses, which normally needs large dynamic suspension forces.

It is now well accepted that suitable advanced vehicle suspension system can best be achievable with the use of active control system. The active suspension can provide a trade off between conflicting requirements by exerting appropriate actuation forces. Use of optimal control theory for designing advanced vehicle suspension systems were suggested by Davis and Thompson (1998), Rutledge (1990), Krtolica and Hrovat (1992), William (1995), Kim (1997), Zaremba, et al. (1997) and Yu and Crolla (1998). However even with active suspension, the limitation remains that the servo control system must react very quickly to suppress disturbances that already have been encountered by the vehicle.

Recently the potential application of preview control in advance suspension design has attracted interest. Bender (1968) proposed the idea of feed-forward control and used the Wiener filter technique to develop the optimal control law for a single-degree-of-freedom vehicle model. Tomizuka (1974, 1975, 1976) described how the preview control could be implemented in practice. Sasaki et al. (1976), Iwata and Nakano (1976) considered a two-dimensional half-car model, which is supported by front and rear suspensions, and studies both heave and pitch motions. Thompson et al. (1980) used a state space approach and linear quadratic regulator theory, and posed the optimal suspension design with preview controller for a quarter-car model. Foag and Grubel (1987) assumed single scalar performance index as an adequate measure of system performance for a half-car model. Hrovat (1991) concluded that the preview suspension control is most appropriate for vehicle moving at high speeds on rough roads.

Yoshimura and Ananthanarayana, (1991) used estimated state variables and the dynamic behavior of the irregular surface for the stochastic optimal control with preview. Experimental confirmation of the effectiveness of the preview (feedforward) control of active suspension system of a test vehicle was reported by Nagiri et al. (1992). Hac (1992), and Hac and Youn (1992, 1993) obtained general analytical solutions including the effects of preview information on ride comfort, road holding, working space of the suspension and power requirements. Huisman et al. (1993) applied a step function as road input and observed reduction in working space and maximum absolute acceleration of the sprung mass. Yeh and Tsao (1994) studied a fuzzy preview control scheme and reported improved suspension performance. Sharp and Pilbeam (1994) augmented a half-car model by a Pade filter to represent the wheel base travel time, and developed control laws, which minimize cost indices containing various weighting constants. Porkop and Sharp (1994) presented a refined approach for the implementation of preview control in discrete time with multiple preview inputs.

Senthil and Norayanan (1996) applied an optimal preview control algorithm to a two-degree-of-freedom vehicle model traveling with constant velocity on a randomly profiled road. They modeled road surface elevation as a homogenous first order filtered white noise random process. Pilbeam and Sharp (1996) reported that the optimal preview control requires comparatively less power consumption. El-Demerdash and Crolla (1996) studied

the effect of component non-linearity on the ride performance of a hydro-pneumatic slow-active suspension and used Pade approximation technique to represent the preview time. Van der Aa and Muijderman (1997) considered two approaches to incorporate constraints on damper range, tire force and suspension travel in the design of controllers to minimize peak values in the chassis acceleration. Mehra et al. (1997) reported substantial improvements in the ride and road holding qualities of vehicle over realistic terrain with the use of active suspension with a preview control. Using half-car model Thompson and Pearce (1998) described the effects of preview on the performance for step type road input, and Marzbanrad et al. (2002) studied the stochastic optimal preview control for filtered white noise road excitations. Marzbanrad et al. (2000) used a three dimensional vehicle model and studied active and preview control system. They used preview information of a hole/bump road and optimal control algorithm with respect to the ride comfort and the road holding.

In this work, a comparative study of active suspensions for three-dimensional seven-degree-of-freedom vehicle traveling on a random road is performed. Different filtered white noise models for the road are used in the analysis and particular attention was given to the preview control system. It is assumed that two non-contact sensors are affixed to the front bumper of the vehicle to provide preview information on the road surface elevations at short distances in the front of the left and right wheel of the vehicle. The effectiveness of optimal active suspensions with respect to ride comfort and road holding preferences for different rough road stochastic models are analyzed. The look-ahead preview and the delay between the front and the rear wheels are included in the analysis. The suspension performances for active, active and delay between the front and the rear wheels, and active and preview control for different road excitations are evaluated and the results are compared with for the passive system. In addition, sensitivity analysis of the control performance to preview time and vehicle load variation is also performed.

2. ROAD ROUGHNESS MODELS

Road surface profiles are commonly measured and recorded in time domain or Fourier analyzed and are characterized by their frequency contents (Heath, 1987). Several models for simulation of road surface profiles were reported in the literature (Heath, 1989; Robson, 1979; Ruf, 1978; Cebon and Newland, 1983). In this section, four types of deterministic and stochastic road models that are used in this study are outlined and their time domain simulation procedures are described.

The simplest model assumes that the road surface is a stationary first order filtered white noise stochastic process with the spectral density

$$S_w(\omega) = \frac{\sigma^2}{\pi} \frac{av}{\omega^2 + (av)^2} \quad (1)$$

where v is the vehicle forward velocity (m/s), ω is the circular frequency (rad/s) and a , σ are constant parameters that depend on the type of the road surface. Here paved road with $a = 0.15 \text{ m}^{-1}$ and $\sigma^2 = 9 \times 10^{-6} \text{ m}^2$ is assumed. The road surface elevation process, $w(t)$, described by the spectral density (1) can be generated by passing a white noise process through a first order filter given as

Table 1. Parameters of the third order filtered white noise road model.

Road type	$\alpha_1 (m^{-1})$	$\alpha_2 (m^{-1})$	$\beta (m^{-1})$	$\sigma_1^2 (m^2)$	$\sigma_2^2 (m^2)$
Paved	0.5	0.2	2.0	2.55×10^{-4}	4.5×10^{-3}

$$\dot{w} + avw = \zeta \quad (2)$$

where $\zeta(t)$ is a Gaussian white noise process with intensity of $2\sigma av$.

Rill (1988) suggested a second order road roughness model that has a power spectral density (PSD) function,

$$S_w(\omega) = Rv \frac{\omega^2 + v^2 \left(\frac{\varphi_1^2 + \alpha \varphi_2^2}{1 + \alpha} \right)}{\omega^4 + (\varphi_1^2 + \varphi_2^2) v^2 \omega^2 + \varphi_1^2 \varphi_2^2 v^4} \quad (3)$$

where φ_1 and φ_2 are road roughness parameter which are assumed to be 0.45 m^{-1} and 0.45 m^{-1} , respectively, for a paved road, and R (m) corresponds to the road surface irregularity height. The corresponding second-order filter white noise for the time domain simulation of the road roughness is given by

$$\ddot{w} + a_1 \dot{w} + a_2 w = \dot{\zeta} + a_3 \zeta \quad (4)$$

where

$$a_1 = (\varphi_1 - \varphi_2) v \quad a_2 = \varphi_1 \varphi_2 v^2 \quad a_3 = \left(\frac{\varphi_1^2 + \alpha \varphi_2^2}{1 + \alpha} \right)^{1/2} v \quad (5)$$

Here $\zeta(t)$ is a Gaussian white noise process with intensity of $v\varphi$.

Recently, a more detailed power spectral density for the road surface roughness was suggested by Rotenberg (1972). i.e.,

$$S(\omega) = (\sigma_1^2/\pi) [\alpha_1 v / (\omega^2 + \alpha_1^2 v^2)] + (\sigma_2^2/\pi) \times [\alpha_2 v (\omega^2 + \alpha_2^2 v^2 + \beta^2 v^2)] / [(\omega^2 + \alpha_2^2 v^2 - \beta^2 v^2)^2 + 4\alpha_2^2 \beta^2 v^4] \quad (6)$$

where $\alpha_1, \alpha_2, \beta, \sigma_1^2, \sigma_2^2$ are coefficients the values of which depend on the type of road/train. The values of parameters for the paved roads as suggested by Rotenberg (1972) are listed in Table 1. The time history of the road elevation with the spectral density given by (6) can be generated by passing a white noise process through a linear third-order filter. That is

$$\ddot{w} + (a_1 + a_3) \dot{w} + (a_0 + a_1 a_3) w = d_1 (\ddot{\zeta} + b_3 \dot{\zeta} + b_0 \zeta) \quad (7)$$

where

$$\begin{aligned}
 a_0 &= -(\alpha_2^2 + \beta^2) v^2 & a_1 &= \alpha_1 v & a_2 &= 2(\alpha_2^2 - \beta^2) v^2 & a_3 &= (a_2 + 2a_0)^{1/2} \\
 b_0 &= -\left[\sigma_1^2 \alpha_1 (\alpha_2^2 + \beta^2)^2 + \sigma_2^2 \alpha_1^2 \alpha_2 (\alpha_2^2 + \beta^2)\right]^{1/2} v^{5/2} / b_4^{1/2} \\
 b_2 &= \left[2\sigma_1^2 \alpha_1 (\alpha_2^2 - \beta^2)^2 + \sigma_2^2 \alpha_2 (\alpha_1^2 + \alpha_2^2 + \beta^2)\right] v^3 / b_4 \\
 b_3 &= (b_2 + 2b_0)^{1/2} & b_4 &= (\sigma_1^2 \alpha_1 + \sigma_2^2 \alpha_2) v & d_1 &= (b_4 / \pi)^{1/2}
 \end{aligned} \tag{8}$$

Here $\zeta(t)$ is a unit intensity Gaussian white noise process.

Figure 1 shows power spectral density of the three filtered white noise stochastic road models as a function of angular frequency, ω , and vehicle velocity, v . It is seen that the power spectral density becomes flatter at low frequencies with increasing the filter order. The first and second filter show a smoothly decaying variation with frequency, while the third order filter has a peak at a frequency that changes with the car speed.

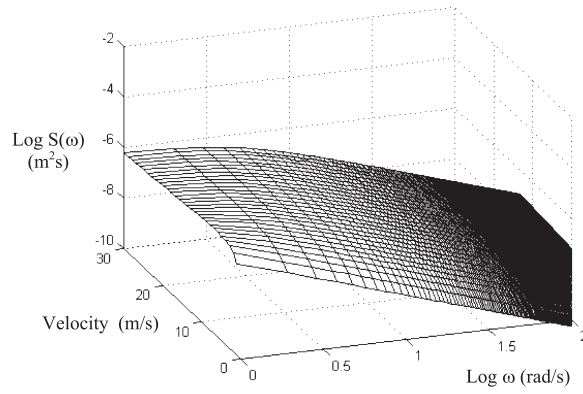
Figure 2 shows the variation of power spectral densities for a vehicle velocity of 20 m/s. It is seen that the spectrum for the third order filter is roughly uniformly at low frequencies and has a peak at angular frequency of 50 rad/s (8 Hz) and then decays smoothly at higher frequencies. The spectra of second and first order filters are roughly constant for angular frequencies below 4 rad/s (0.64 Hz) and 1 rad/s (0.16 Hz), respectively, and then decay with further increase in the frequency.

In addition to the stochastic models, a haversine type hole followed by a bump in the road is also studied. In this case, the road profile is given as

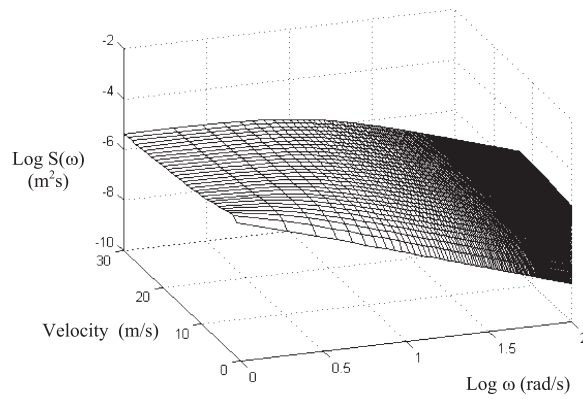
$$w(t) = \begin{cases} h [1 - \cos \omega_r (t - t_0)] & \text{for } t \in [t_0, t_r] \\ 0 & \text{otherwise} \end{cases} \tag{9}$$

Here h is the height of the hole or the bump, t is the time, $\omega_r = 2\pi v/D$, where v is vehicle velocity and D is the width of the hole or bump. In Equation (9), t_0 and $t_r = t_0 + D/v$ are, respectively, the time that the front tire reaches the hole or the bump and passes it. In this study, $h = 0.1$ m, $v = 20$ m/s and $D = 0.5$ m, are used.

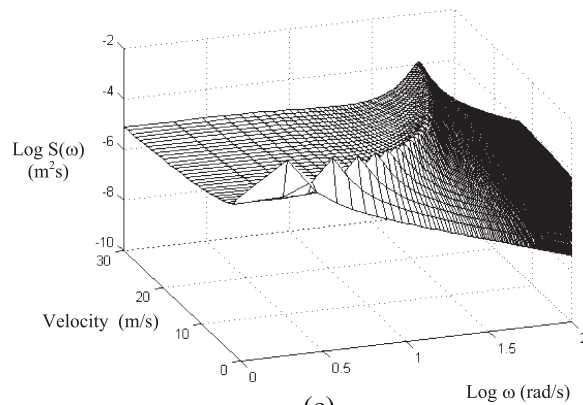
For a vehicle speed of 20 m/s, sample time histories of road profiles generated by different models are compared in Figure 3. This figure shows that the time histories of first and second filtered white noise model show a random pattern, while that of the third order filter shows a noticeable frequency of about 6 to 8 Hz. While the rough surface waves are fixed in space, the frequency content of the road excitation will vary depending on the vehicle velocity. In Figure 3, the hole/bump curve is a 0.5 m long hole with a height of 0.1 m followed by a 0.5 long bump for the vehicle speed of 20 m/s. The hole/bump length will change in direct proportion with the vehicle speed.



(a)



(b)



(c)

Figure 1. Power spectral density functions of stochastic road surface models as functions of frequency and vehicle velocity. (a) First order filter model. (b) Second order filter model. (c) Third order filter model.

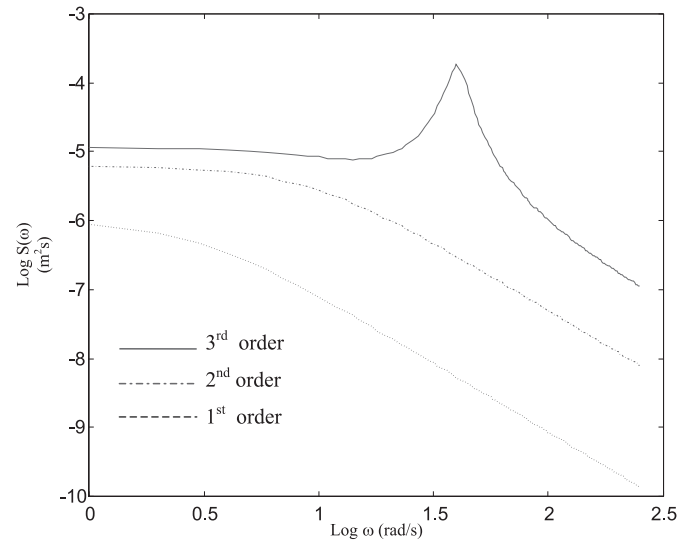


Figure 2. Power spectral density functions of different stochastic road models for the vehicle velocity of 20 m/s.

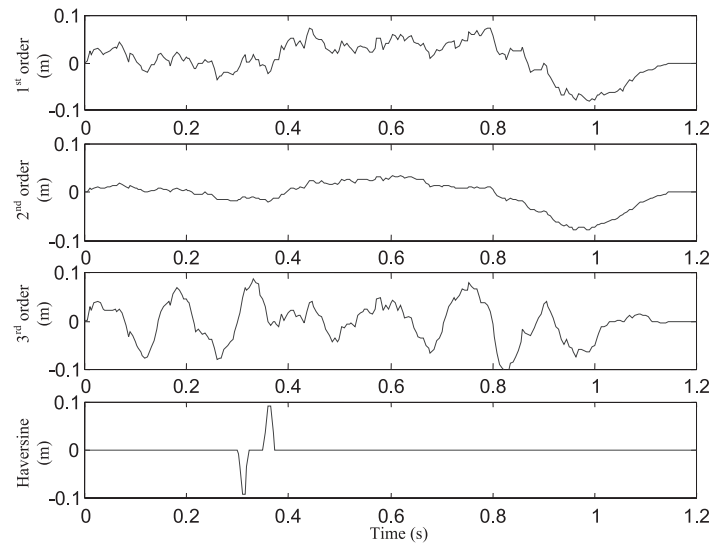


Figure 3. Sample time histories of simulated road profiles for $v = 20$ m/s.

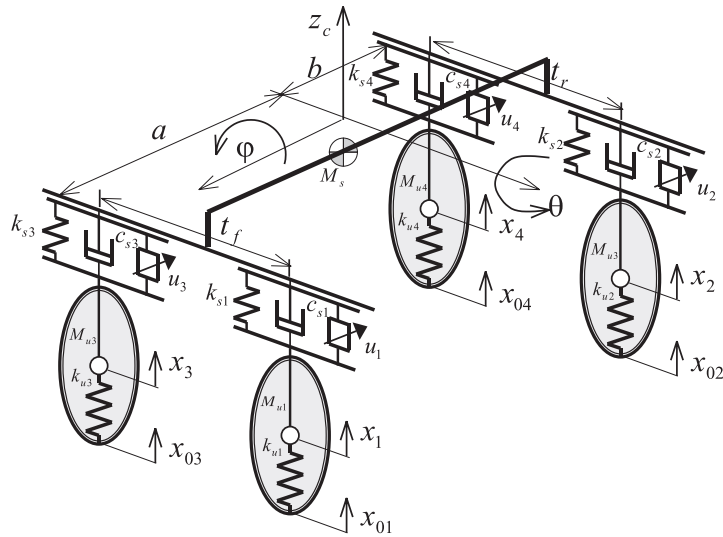


Figure 4. Mechanical model of vehicle suspension system.

3. VEHICLE SYSTEM FORMULATION

3.1. Suspension Model

In this study, a full-car model with seven degrees of freedoms is considered. Figure 4 shows the schematics of the model used. The three dimensional model contains three degrees of freedom for the sprung mass (bouncing, rolling and pitching) and four degrees of freedom for the vertical motions of the front and the rear unsprung masses. It is assumed that the rear tires travel over the same path as the front tires; hence x_{02} is a delayed version of x_{01} . i.e., $x_{02} = x_{01}(t - t_d)$, and x_{04} is a delayed version of x_{03} , $x_{04} = x_{03}(t - t_d)$ where $t_d = v/(a + b)$ is the delay time between the front and the rear wheel, v is the forward vehicle speed and $a + b$ is the vehicle wheel base. Assuming the pitch and roll motion are small and the characteristics of all passive suspension elements are linear, the equations of motion as evaluated by Marzbanrad et al. (2001) are given as

$$\begin{aligned}
 & M_{u1} \ddot{x}_1 + c_{s1} \dot{x}_1 + (k_{u1} + k_{s1}) x_1 - k_{u1} x_{01} - c_{s1} (\dot{x}_5 - a \dot{x}_6 + 0.5 t_f \dot{x}_7) \\
 & - k_{s1} (x_5 - a x_6 + 0.5 t_f x_7) + u_1 = 0 \\
 & M_{u2} \ddot{x}_2 + c_{s2} \dot{x}_2 + (k_{u2} + k_{s2}) x_2 - k_{u2} x_{02} - c_{s2} (\dot{x}_5 + b \dot{x}_6 + 0.5 t_r \dot{x}_7) \\
 & - k_{s2} (x_5 + b x_6 + 0.5 t_r x_7) + u_2 = 0
 \end{aligned}$$

$$\begin{aligned}
& M_{u3}\ddot{x}_3 + c_{s3}\dot{x}_3 + (k_{u3} + k_{s3})x_3 - k_{u3}x_{03} - c_{s3}(\dot{x}_5 - a\dot{x}_6 - 0.5t_f\dot{x}_7) \\
& - k_{s3}(x_5 - ax_6 - 0.5t_fx_7) + u_3 = 0 \\
& M_{u4}\ddot{x}_4 + c_{s4}\dot{x}_4 + (k_{u4} + k_{s4})x_4 - k_{u4}x_{04} - c_{s4}(\dot{x}_5 + b\dot{x}_6 - 0.5t_r\dot{x}_7) \\
& - k_{s4}(x_5 + bx_6 - 0.5t_rx_7) + u_4 = 0 \\
& M_s\ddot{x}_5 + (c_{s1} + c_{s2} + c_{s3} + c_{s4})\dot{x}_5 + (k_{s1} + k_{s2} + k_{s3} + k_{s4})x_5 \\
& + (-ac_{s1} + bc_{s2} - ac_{s3} + bc_{s4})\dot{x}_6 + (-ak_{s1} + bk_{s2} - ak_{s3} + bk_{s4})x_6 \\
& - c_{s1}\dot{x}_1 - c_{s2}\dot{x}_2 - c_{s3}\dot{x}_3 - c_{s4}\dot{x}_4 - k_{s1}x_1 - k_{s2}x_2 - k_{s3}x_3 - k_{s4}x_4 \\
& - (u_1 + u_2 + u_3 + u_4) = 0 \\
& I_{yy}\ddot{x}_6 + (-ac_{s1} + bc_{s2} - ac_{s3} + bc_{s4})\dot{x}_5 + (-ak_{s1} + bk_{s2} - ak_{s3} + bk_{s4})\dot{x}_5 \\
& + (a^2c_{s1} + b^2c_{s2} + a^2c_{s3} + b^2c_{s4})\dot{x}_{6s3} + (a^2k_{s1} + b^2k_{s2} + a^2k_{s3} + b^2k_{s4})x_6 \\
& + ac_{s1}\dot{x}_1 - bc_{s2}\dot{x}_2 + ac_{s3}\dot{x}_3 - bc_{s4}\dot{x}_4 + ak_{s1}x_1 - bk_{s2}x_2 + ak_{s3}x_3 - bk_{s4}x_4 \\
& + au_1 - bu_2 + au_3 - bu_4 = 0 \\
& I_{xx}\ddot{x}_7 + 0.25(t_f^2c_{s1} + t_r^2c_{s2} + t_f^2c_{s3} + t_r^2c_{s4})\dot{x}_7 \\
& + 0.25(t_f^2k_{s1} + t_r^2k_{s2} + t_f^2k_{s3} + t_r^2k_{s4})x_7 \\
& + 0.5(-t_fc_{s1}\dot{x}_1 - t_rc_{s2}\dot{x}_2 + t_fc_{s3}\dot{x}_3 + t_rc_{s4}\dot{x}_4) \\
& + 0.5(-t_fk_{s1}x_1 - t_rk_{s2}x_2 + t_fk_{s3}x_3 + t_rk_{s4}x_4) \\
& + 0.5(-t_fu_1 - t_ru_2 + t_fu_3 + t_ru_4) = 0
\end{aligned} \tag{10}$$

where x_1, x_2, x_3 , and x_4 are the vertical displacement of the unsprung masses, x_5 is the vertical displacement of the center of gravity of the sprung mass, x_6 is the pitch motion of the sprung mass, and x_7 is the roll motion of the sprung mass. Other parameters are defined in Figure 4, and are listed in Table 2.

Equations (10) can be expressed in state space form as

$$\dot{x} = Ax + Bu + Ew, \quad x_0(t_0) = x_0 \tag{11}$$

where A, B , and E are constant matrices of dimensions 14×14 , 14×4 , and 14×4 , respectively. In (11), the state, the control input and the disturbance input vectors are given as

Table 2. Parameters of the vehicle model.

SPRUNG MASS		UNSPRUNG MASS	
<i>Parameters</i>	<i>Values</i>	<i>Parameters</i>	<i>Values</i>
M_s	1460 kg.	M_{u1}, M_{u3}	40.0 kg.
I_{xx}	460 kg.m ²	M_{u2}, M_{u4}	35.5 kg.
I_{yy}	2460 kg.m ²	k_{s1}, k_{s3}	19960 N/m
t_f	1.522 m	k_{s2}, k_{s4}	17500 N/m
t_r	1.510 m	C_{s1}, C_{s3}	1290 N.s/m
a	1.011 m	C_{s2}, C_{s4}	1620 N.s/m
b	1.803 m	$k_{u1} \sim k_{u4}$	175500 N/m

$$x = [x_1, x_2, \dots, x_{14}]^T, \quad u = [u_1, u_2, u_3, u_4]^T, \quad w = [x_{01}, x_{02}, x_{03}, x_{04}]^T \quad (12)$$

Here $x_5 = z_c$, $x_6 = \theta$ and $x_7 = \varphi$ are sprung mass motions and $x_8 \sim x_{14}$ are defined as the derivatives of $x_1 \sim x_7$. Control forces $u_1 \sim u_4$ are supplied by mechanical actuators that are activated independently.

3.2. Performance Index

The performance of the suspension system is to be optimized with respect to ride comfort, suspension rattle space, and road holding. The performance index should, therefore, include the mean square values of i) the body acceleration, ii) relative displacement between the body and the wheel, and iii) the dynamic tire force, which is proportional to the wheel-to-road displacement. In addition, the magnitude of the active control force should be minimized. Here the performance index to be minimized is assumed to be given as

$$\begin{aligned}
 J = & \lim_{2T} \frac{1}{2T} \int_0^T \begin{bmatrix} 1 \\ \ddot{z}_c \\ \ddot{\theta} \\ \ddot{\varphi} \end{bmatrix}^T \begin{bmatrix} 0 & 0 & 0 & 0 \\ 0 & \rho_1 & 0 & 0 \\ 0 & 0 & \rho_2 & 0 \\ 0 & 0 & 0 & \rho_3 \end{bmatrix} \begin{bmatrix} 1 \\ \ddot{z} \\ \ddot{\theta} \\ \ddot{\varphi} \end{bmatrix} \\
 & + \begin{bmatrix} s_1 \\ s_2 \\ s_3 \\ s_4 \end{bmatrix}^T \begin{bmatrix} \rho_4 & 0 & 0 & 0 \\ 0 & \rho_5 & 0 & 0 \\ 0 & 0 & \rho_6 & 0 \\ 0 & 0 & 0 & \rho_7 \end{bmatrix} \begin{bmatrix} s_1 \\ s_2 \\ s_3 \\ s_4 \end{bmatrix} \\
 & + \begin{bmatrix} t_1 \\ t_2 \\ t_3 \\ t_4 \end{bmatrix}^T \begin{bmatrix} \rho_8 & 0 & 0 & 0 \\ 0 & \rho_9 & 0 & 0 \\ 0 & 0 & \rho_{10} & 0 \\ 0 & 0 & 0 & \rho_{11} \end{bmatrix} \begin{bmatrix} t_1 \\ t_2 \\ t_3 \\ t_4 \end{bmatrix}
 \end{aligned}$$

$$+ \begin{bmatrix} u_1 \\ u_2 \\ u_3 \\ u_4 \end{bmatrix}^T \begin{bmatrix} \rho_{12} & 0 & 0 & 0 \\ 0 & \rho_{13} & 0 & 0 \\ 0 & 0 & \rho_{14} & 0 \\ 0 & 0 & 0 & \rho_{15} \end{bmatrix} \begin{bmatrix} u_1 \\ u_2 \\ u_3 \\ u_4 \end{bmatrix} \quad (13)$$

where

$$\ddot{z} = \ddot{x}_5 = \dot{x}_{12}, \quad \ddot{\theta} = \ddot{x}_6 = \dot{x}_{13}, \quad \ddot{\varphi} = \ddot{x}_7 = \dot{x}_{14} \quad (14)$$

and

$$\begin{aligned} s_1 &= x_5 - x_1 + 0.5t_f x_7 - ax_6, & s_2 &= x_5 - x_2 + 0.5t_f x_7 + bx_6 \\ s_3 &= x_5 - x_3 + 0.5t_f x_7 - ax_6, & s_4 &= x_5 - x_4 - 0.5t_f x_7 + bx_6 \\ t_1 &= x_1 - x_{01}, & t_2 &= x_2 - x_{02}, & t_3 &= x_3 - x_{03}, & t_4 &= x_4 - x_{04} \end{aligned} \quad (15)$$

For expressing the performance index in a form that is quadratic in the state and input vectors, it is required to substitute the acceleration \ddot{z} , $\ddot{\theta}$ and $\ddot{\varphi}$, and variables s_i and t_i from Equations (10), (14) and (15), in Equation (13) with using state Equation (11) and notation (12) to have

$$J = \lim_{T \rightarrow \infty} \frac{1}{2T} \int_0^T (x^T Q_1 x + 2x^T N u + u^T R u + 2x^T Q_{12} w + w^T Q_2 w) dt \quad (16)$$

where Q_1 , N , R , Q_{12} and Q_2 are time-invariant weighting matrices. Q_1 , R and Q_2 are symmetric and $Q_n = Q_1 - R^{-1}N^T$ is semi-positive matrix.

Choosing the weighting constants $\rho_1 \sim \rho_{14}$ in (13) depends on designer's preferences. When it is desired to decrease the sprung mass accelerations, the pertinent weights, ρ_1, ρ_2, ρ_3 , should be increased compared to others. On the other hand, when the emphasis is on the stability, $\rho_4 \sim \rho_{11}$ should be increased. With increasing $\rho_{12} \sim \rho_{15}$, the magnitude of the actuator forces can be reduced. Since the performance index contains parameters with different units, the weighting constants listed in Table 2 must be selected with proper units such that the performance index is nondimensionalized. In addition, the weighting constants must be chosen such that the positive semi-definite condition for matrix Q_n in (16) is satisfied. In this study, two set of weighting constants, respectively, for road holding and ride comfort preferences are considered.

3.3. Optimal Preview

It is assumed that the road excitation input $w_1(\tau)$ and $w_3(\tau)$ for $\tau \in [t, t + t_p]$ is measured by the preview sensors at the front bumper. That is, the preview information about the ground excitation $w(t)$ up to t_p ahead of current time t is available. In addition, for rear wheels the input $w_2(\tau)$ and $w_4(\tau)$ are known for $\tau \in [t, t + t_p + t_d]$. The method for

developing a continuous time optimal preview control law for systems with multiple inputs were described by Hac (1992), Hac and Youn (1993) and Marzbanrad (2001). Their main result is summarized in this section.

Problem Statement. Consider a system that is governed by the state space equation given by (11) and with preview time t_p on the excitation $w(t)$ (i.e., $w(\sigma), \sigma \in [t + t_p]$ is known.) The optimal preview control problem reduces to finding a control law $u(t) = f(x(t), w(\sigma), \sigma \in [t + t_p])$ that minimizes the quadratic performance index given by (16).

Now let

$$A_n = A - BR^{-1}N^T, \quad Q_n = Q_1 - NR^{-1}N^T \quad (17)$$

and assume that Q_n is nonnegative definite, and $Q_n = T^T T$; then if the pair (A_n, B) is stabilizable and the pair (A_n, T) is detectable, the optimal preview control law is given by

$$u(t) = -R^{-1} [(N^T + B^T P)x(t) + B^T r(t)] \quad (18)$$

where P is the positive definite solution of the Algebraic Riccati equation

$$PA_n + A_n^T P - PBR^{-1}B^T P + Q_n = 0 \quad (19)$$

and the vector $r(t)$ is given by

$$r(t) = \int_0^{t_p + t_d} e^{A_c^T \sigma} (PD + Q_{12}) \begin{bmatrix} H(t_p - \sigma) w_1(t + \sigma) \\ w_1(t + \sigma - t_d) \\ H(t_p - \sigma) w_3(t + \sigma) \\ w_3(t + \sigma - t_d) \end{bmatrix} d\sigma \quad (20)$$

where

$$H(t_p - \sigma) = \begin{cases} 1 & \text{for } \sigma \leq t_p \\ 0 & \text{for } \sigma > t_p \end{cases} \quad (21)$$

where A_c is the close loop system matrix given by

$$A_c = A - BR^{-1}(N^T + B^T P) = A_n - BR^{-1}B^T P \quad (22)$$

A_c must have eigenvalues with negative real parts, so that the system remain asymptotically stable. Consequently, the exponential function in Equation (20) will decrease with time and hence, the integral defining $r(t)$ places more emphasis in the preview control law on the input in the near future than on that further ahead in time.

The optimal control $u(t)$ given by (18) consists of two terms. The first term is the feedback part, which is the identical to that for an optimal control in the absence of preview sensors. The second term is the feed-forward part, which takes advantage of the preview information available.

In this study, the performance of the suspension for the cases of passive, active, active and delay, and active and preview are analyzed. The active case is when no preview information is available. The active and delay case, uses the preview control of the rear wheels based on

the contact information of the front wheels. For active and preview case, preview sensors are assumed to be attached to the vehicle front bumper that provide information of the road surface height ahead of the car so that preview control of both the front and rear wheels can be achieved. In this case, $t_p = l/v$, where l is the preview distance that the front sensors can look ahead.

3.4. Power Demand

For active systems, the applied control forces, $u_i, i = 1 \sim 4$ in Equation (11) are assumed to be developed by four independent actuators in parallel with the mechanical springs and shock absorbers as shown in Figure 4. The power consumption of the actuators together and with damper system is given by

$$P_i = (c_{si} \dot{s}_i - u_i) \dot{s}_i, \quad i = 1, 2, 3, 4 \quad (23)$$

This including active control force and power dissipated by the damper. For the passive system the power loss is given by the first term in Equation (23). In practice, the mean-square power demand, $E(P_i^2)$, is used as a measure of energy consumption for comparing different cases.

4. RESULTS AND DISCUSSIONS

In this section, the results of the active control of a full car model traveling on different types irregular roads are described. The performance of passive and active suspension systems are evaluated and compared. For the case of preview active control, it is assumed two non-contact sensors are mounted on front bumpers that provide information of the road ahead and the full state of the system is used in the optimal active control strategy. The vehicle parameters suggested by Chalasani (1986) for a four-door sedan car that are used in analysis are listed in Table 2. In this case the natural frequencies of the vehicle suspension are 1, 1.3, 1.5, 11.1, 11.1, 11.7, and 11.7 Hz. The first three frequencies correspond to the sprung mass vertical, roll and pitch vibration modes, respectively. The other four frequencies are for the front and the rear wheel vertical vibrations. Two sets of weighting constants used in performance index (13), which are respectively for the ride comfort and the road holding, are in Table 3. In this table the closed loop system poles are also listed for completeness.

4.1. Vehicle Response

For active suspensions, the weighting constants for the ride comfort preference are selected and the accelerations of center of gravity of sprung mass are computed. Figure 5 compares the acceleration responses for passive, active, active and delay, and active and preview suspensions. In the case of active and delay, it is assumed that the rear tire use the preview information from its front tire, but the front tire does not have any preview data. In the case of active and preview control, the front tire also receives information from the front bumper sensors about the road irregularities ahead of the vehicle. Unless stated otherwise, a preview

Table 3. Weighting constants for ride comfort and road holding and the corresponding closed loop system poles.

Ride comfort			Road holding		
weighting constants		eigenvalues	weighting constants		eigenvalues
1	3	$-28.22 + 72.25i$	1	3	$-67.17 + 94.50i$
2	8	$-28.22 - 72.25i$	2	8	$-67.17 - 94.50i$
3	1	$-10.77 + 67.53i$	3	1	$-33.24 + 74.65i$
4	1200	$-10.77 - 67.53i$	4	18000	$-33.24 - 74.65i$
5	1400	$-9.23 + 70.13i$	5	19500	$-25.55 + 71.73i$
6	1200	$-9.23 - 70.13i$	6	18000	$-25.55 - 71.73i$
7	1400	$-8.59 + 67.64i$	7	19500	$-25.26 + 73.56i$
8	12000	$-8.59 - 67.64i$	8	200000	$-25.26 - 73.56i$
9	11000	$-5.31 + 6.14i$	9	195000	$-8.07 + 9.80i$
10	12000	$-5.31 - 6.14i$	10	200000	$-8.07 - 9.80i$
11	11000	$-4.00 + 5.07i$	11	195000	$-7.14 + 8.76i$
12	1e-6	$-4.00 - 5.07i$	12	1e-6	$-7.14 - 8.76i$
13	1e-6	$-3.51 + 4.52i$	13	1e-6	$-5.48 + 7.09i$
14	1e-6	$-3.51 - 4.52i$	14	1e-6	$-5.48 - 7.09i$
15	1e-6		15	1e-6	

time of 0.12 second for a vehicle with travelling velocity of 20 m/s is used in the analysis. The simulation is also performed for a time duration of 1.2 second.

Sample vehicle accelerations in vertical, pitch and roll motions are shown in Figures 5. Here it is assumed that the left wheels of the car encounter a rough road that is represented by a third order filtered white noise model as given by Equation (7). This figure shows that in addition to vertical and pitch accelerations, roll acceleration also appears in the vehicle body due to uneven excitations. It is of interest to point out that the car roll motion is completely ignored when a full-car model is not used.

Figure 5 shows that the acceleration amplitudes for the active suspension with preview are generally lower than other active and passive systems. When the preview information is available, the control actuators react to the anticipated road irregularities. The preview information help the active system to reduce the force transmitted to the vehicle body and consequently leading to smoother ride and improved tracking of the road.

The corresponding time histories of wheel tracking of the suspension system, $x_i, i = 1, \dots, 4$, are shown in Figure 6. The road surface variation is also shown by dashed lines in this figure for comparison. It is observed that the preview controller activates the actuators before the wheels encounter the road unevenness. Front wheel of the vehicle with active and preview control systems reacts before the other wheels because it observes or encounters the road roughness first. The rear wheel begins to respond when their corresponding front wheel encounters the road unevenness for the preview control and active and delay systems. It is clearly observed that the wheel tracking pursues road unevenness. Additional results (not shown here due to space limitation) for the road holding preference show that the wheels follow the road much closer than that in the ride comfort preference.

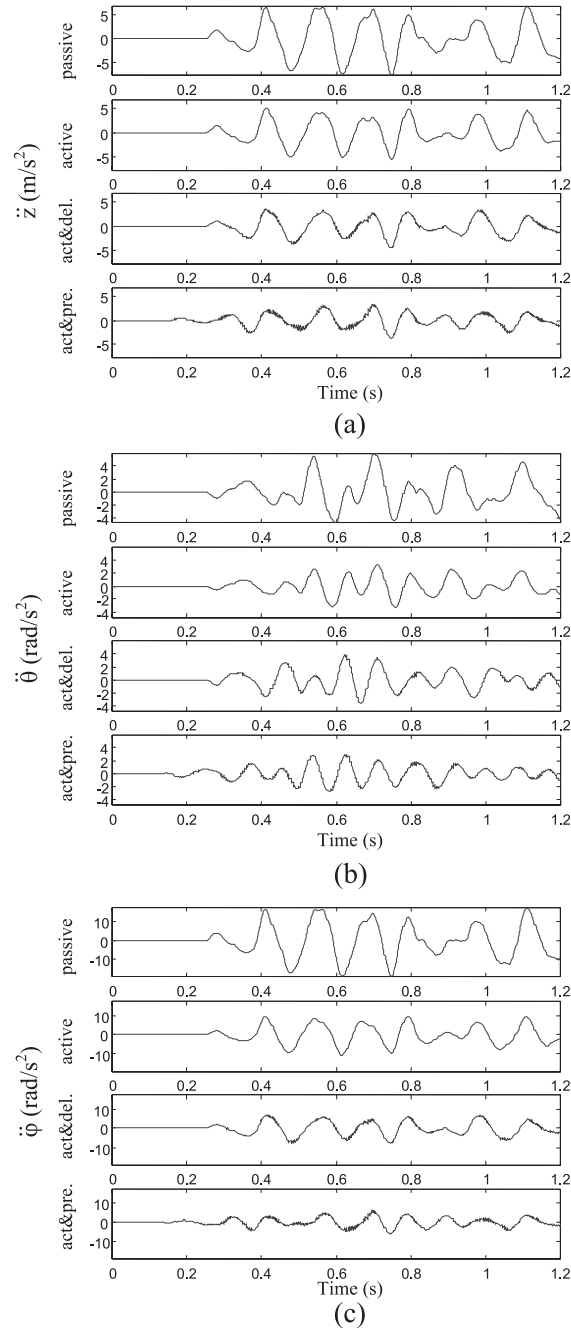


Figure 5. Time histories of accelerations with ride comfort preference when the vehicle left side faces the third order filtered white noise road excitation. (a) Vertical. (b) Pitch. (c) Roll.

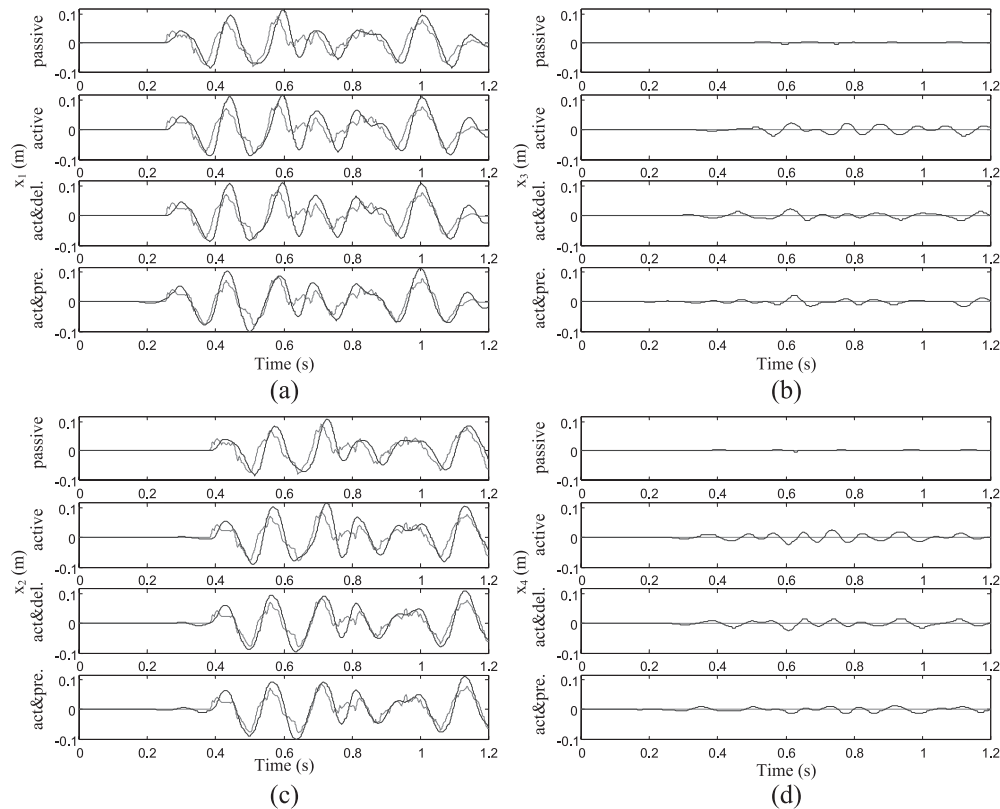


Figure 6. Time histories of wheel tracking with ride comfort preference when the vehicle left side faces the third order filtered white noise road excitation. (a) Front-Left wheel. (b) Front-Right wheel. (c) Rear-Left wheel. (d) Rear-Right wheel.

4.2. Performance

Performance index (13) contains accelerations, suspension rattle spaces, tire deflections, and control forces. Although the goal of the optimal control is to minimize the performance index, J , it is of interest to examine the values of various mean-square parameters separately. This is because while the performance index may be minimized, it is unacceptable to have values of some parameters surpass their practical limitations. Here, the magnitudes of the performance index along with mean square values of different suspension parameters for all four types of road models are evaluated and the results are listed in Tables 4 and 5. All mean-square values are normalized and are presented as percentages of the corresponding values for the passive system. In these tables, it is assumed that only the vehicle left side wheels encounter the road excitations and a fixed preview time of 0.12 second is also used.

Table 4 is for the ride comfort preference and Table 5 is for the road holding. These tables show that the active and preview control suspension not only have the lowest performance index, but also reduces most mean-square parameters as well. Active and delay control

Table 4. Suspension performances for different types of road excitations with ride comfort preference when vehicle left side encounters the road irregularities.

System	$E(\ddot{z}_c^2)$	$E(\ddot{\theta}^2)$	$E(\ddot{\varphi}^2)$	$E(s_1^2)$	$E(s_2^2)$	$E(s_3^2)$	$E(s_4^2)$	$E(t_1^2)$	$E(t_2^2)$	$E(t_3^2)$	$E(t_4^2)$	J
Passive	100	100	100	100	100	100	100	100	100	100	100	100
Road 1												
Active	53.6	43.2	32.9	100.2	134.7	368.6	112.7	123	128.9	193.7	266.2	66.3
Active&Delay	30.5	47.5	19.3	96.4	121.6	107.2	55.3	125.5	77.4	101.5	145.7	56.3
Active&Preview	21.7	37.9	13.9	76.8	174.7	125.8	194.3	77.4	79.1	89.2	93.4	47.6
Road 2												
Active	40.6	36.8	23	74.9	105.6	46.1	25.9	112.9	117	21.2	34.9	50.7
Active&Delay	26.3	38.1	17.3	67.7	98.3	12.9	9.8	110.4	69.3	13	21.7	43.9
Active&Preview	15.3	33.0	11.5	55.8	123.4	18.8	45.8	69.4	70.7	10.6	15.3	36.9
Road 3												
Active	51.1	34.6	30.5	123.6	135.1	889.1	829.4	121.1	108.4	826	793.4	53.7
Active&Delay	27.8	38.2	17.6	119.2	135.3	544.5	577.5	113.2	63.7	559.8	601.7	44.6
Active&Preview	17.8	27.3	8.8	113.2	136.5	392.7	361.3	65.1	68	369.3	356.3	36
Road 4												
Active	66.9	58.2	41.7	144.5	191.3	317	445.4	130.9	145.4	319.8	442.6	83.6
Active&Delay	37.3	64	23.8	157.6	116.1	113.7	196.3	138.2	78.9	119.7	199	69.8
Active&Preview	32.4	54.7	21.9	89.1	116.7	115.2	105.9	77.3	79.5	116.8	104.5	58

Table 5. Suspension performances for different types of road excitations with road holding preference when vehicle left side encounters the road irregularities.

System	$E(\ddot{z}_c^2)$	$E(\ddot{\theta}^2)$	$E(\ddot{\varphi}^2)$	$E(s_1^2)$	$E(s_2^2)$	$E(s_3^2)$	$E(s_4^2)$	$E(t_1^2)$	$E(t_2^2)$	$E(t_3^2)$	$E(t_4^2)$	J
Passive	100	100	100	100	100	100	100	100	100	100	100	100
Active	189.9	130.6	100	134	173.6	344.4	140.5	81.2	80	130.7	263.5	108.4
Active&Delay	162.4	118.1	100	98.2	86.9	550	148.7	74.5	41.1	172.9	224.8	86
Active&Preview	135.5	99.9	89.9	71.8	88.7	235.2	24	28	32.5	23	34.8	54
Road 1												
Active	251.3	163	100	107.3	179.2	68.6	107.3	174.1	75.1	31.4	110.7	129.5
Active&Delay	174.6	117.9	98.8	77.4	53.3	189.3	58	116.5	56.6	44.2	68.2	89.5
Active&Preview	66.4	79.6	56.1	51.5	57.5	47.3	6.9	26.9	31	3.2	8	39.8
Road 2												
Active	165	125.2	100	45.5	60.9	774.1	675.4	63.9	84.5	536.9	574.6	95.5
Active&Delay	129.2	78.1	93.9	41.5	97.5	365.1	612	63.2	20	230.6	567.3	68.5
Active&Preview	86.4	66.9	56.3	77.4	95.7	149.5	157.8	13.8	17.2	89.6	125.2	44.2
Road 3												
Active	159.5	107.1	100	32	54	75.6	118.2	56.8	70.4	66.8	105.6	73.4
Active&Delay	134.1	129.4	90.68	33.75	69.2	22.7	49.5	57.6	36.3	19.6	46.3	61.8
Active&Preview	163.8	126.8	100	45.5	66.8	20	21.2	29.1	35.4	18.8	19	52.6
Road 4												

has better performance when compared with the active control for suspension space and tire deflection of rear tire. Inclusion of time delay reduces the vertical acceleration more effectively than angular accelerations in pitch and roll motion with respect to active system. Based on the results presented in Tables 4 and 5, it appears that the order of effectiveness beyond the preview control is the active and delay, and active suspension systems.

Tables 4 and 5 show that the active suspension can significantly reduce the vertical acceleration, \ddot{z} , with ride comfort, particularly, for active with preview systems. Pitch acceleration, $\ddot{\theta}$, is also markedly reduced for active suspensions for all road models with ride comfort preference. The suspension with active and preview control also reduces the pitch acceleration with road holding preference as well. Roll acceleration, $\ddot{\phi}$, around the longitudinal vehicle axis appears because of the unsymmetrical road excitation. From Table 4, it is observed that the roll acceleration is highly reduced by the active suspension, especially, the one with preview control and the ride comfort preference.

Table 5 summarizes the performance results for the road holding preference. Here, the emphasis is on lowering the tire loads, which are directly proportional to the tire deflections. It is observed the tire deflection in the vehicle left side (encountering the road roughness) reduces significantly by the active systems especially with active preview control. The amount of tire deflections for right side where the road is smooth appear to increase for the active systems when compared with the passive system. However, as seen from Figure 6_{b,d}, the tire deflection for the right side is very small. Therefore, a slight increase in magnitude is acceptable. Table 5 also shows that the suspension with preview control generally reduces the tire deflection for both sides. This is another advantage of the preview control for both preferences.

In this study, four different road models are used to assess the sensitivity of the suspension control systems to the type of road excitation. From Tables 4 and 5 it may be concluded that the performance index and the mean square accelerations of active suspensions have similar trend of variations for these different roads. That is the performance of the active suspension system is not sensitive to the road excitation model used.

Tables 4 and 5 show that the response acceleration for the ride comfort preference is more effectively decreased when compared with those for the road holding preference. In contrast, parameter values for road holding preference that express stability ($t_i, i = 1 \sim 4$) are much less than those corresponding values in ride comfort preference. However, the total performance indices for both ride comfort and road holding preference are approximately the same for different cases.

4.3. Power Consumption

Designing an acceptable suspension system requires consideration of power demand for different road conditions. The total power demand including the power dissipated by the damper and the power consumption of the control system actuators are shown in Table 6. Mean square values of power demand as evaluated by Equation (23) during a period of 1.2 second are evaluated and the results are normalized with corresponding values for the passive systems. In this table, $E\{\}$ denotes the expected value and the normalized mean square responses are presented for both ride comfort and road holding preferences. The road irregularities are assumed to excite the vehicle on both side wheels. Table 6 shows that the

Table 6. Normalized power demand for different types of road excitations when both sides of the vehicle face the road irregularities.

System	$E(P_1^2)$		$E(P_2^2)$		$E(P_3^2)$		$E(P_4^2)$	
	Ride	Road	Ride	Road	Ride	Road	Ride	Road
	co.	ho.	co.	ho.	co.	ho.	co.	ho.
Passive	100	100	100	100	100	100	100	100
Active	83.9	95.7	109.7	107.6	88.6	96.6	107.3	107.6
Road 1 Active&Delay	80.6	95.5	16.1	23.8	80.7	97.1	16.9	24.1
Active&Preview	12.5	31.7	14.2	22.9	10.8	31.5	15	23.3
Active	69.9	159.5	91.6	116.8	85.5	163.6	79.1	115.4
Road 2 Active&Delay	84.2	161.5	15.8	17.5	76	166.9	17	17.8
Active&Preview	22.3	25.1	13.4	16.2	16.8	25.1	13.4	16.8
Active	94.2	86.8	73.1	83.9	98.2	87.2	69.3	82.8
Road 3 Active&Delay	89.7	85.7	11	19.9	90.1	84.7	11.7	19.8
Active&Preview	12.4	28.8	10.7	20.8	12.8	28.6	11.3	20.7
Active	103.3	71.1	142.5	100.5	103.8	71.1	141.7	100.5
Road 4 Active&Delay	95.7	69.1	29.3	26.8	98.2	70.1	32.3	27.4
Active&Preview	16.2	21.9	22.9	27.1	16.3	22.2	25.9	27.6

power demands for different road models follow the same pattern of variations for both ride comfort and road holding preferences. It is also seen that the active and preview control decreases the power consumption for both preferences.

4.4. Sensitivity Analysis

For sensors that provide information at a fixed distance ahead of the vehicle, the preview time changes with the vehicles speed. In addition, the number of passengers or the load carried by the vehicle changes the mass of vehicle body. In this section, the sensitivity of preview active system with respect to the preview time and sprung mass is studied.

Figure 7 shows the effect of preview time in the range of 0.01 to 0.19 seconds on the mean-square accelerations and performance index. In this figure, the performance index and the mean-square accelerations are normalized with respect to the case of active control with out preview (i.e., $t_p = 0$). It should be emphasized that when the sensors can see a fixed distance ahead, the preview time depends on the vehicle speed. When the bumper sensors observe 2.4 m ahead and the vehicle speed is 20 m/s (72 Km/h), the preview time is 0.12 second. Figure 7 shows that the performances reach to smooth values after about 0.1 second for ride comfort preference and after 0.04 second for road holding preference. It is also observed that additional increase in the preview time does not produce significant improvement in the performance index. This is because $r(t)$ as defined by Equation (20) is not significantly affected by an increase in t_p , due to the exponentially decaying term in the integral (with exponent depending on the closed loop matrix, A_c , which is asymptotically stable).

The mass of vehicle varies when load carried by the vehicle changes. (e.g., as number of passengers varies.). Figure 8 shows the variation of the performance index with sprung

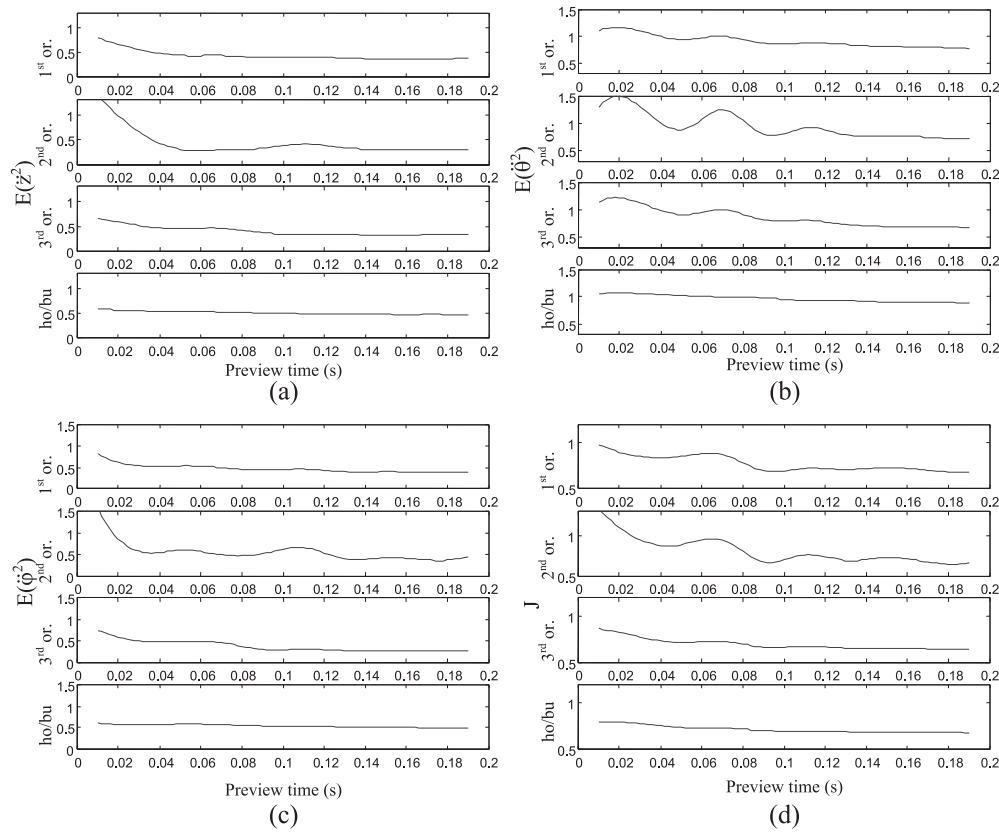


Figure 7. The effect of preview time on normalized performance for different road models with ride comfort preference. (a) Vertical acceleration. (b) Pitch acceleration. (c) Roll acceleration. (d) Total performance index.

mass. The performance indices are evaluated for different active suspensions and for various road models. Here, the performance indices are given as percentages of the corresponding passive system. The performance of various active suspensions for different road models can also be compared in this figure.

Considering 1460 kg for the body of vehicle as shown in Table 2, it is assumed to load the vehicle up to 2000 kg. It is clearly observed that for all roads there is no sensible altering for this boundary. The results also show that the performance index decreases from active, to active and delay, and to active and preview system. This is true for all type road models, however, the performance index of these three active control systems are different according to the type of road input model.

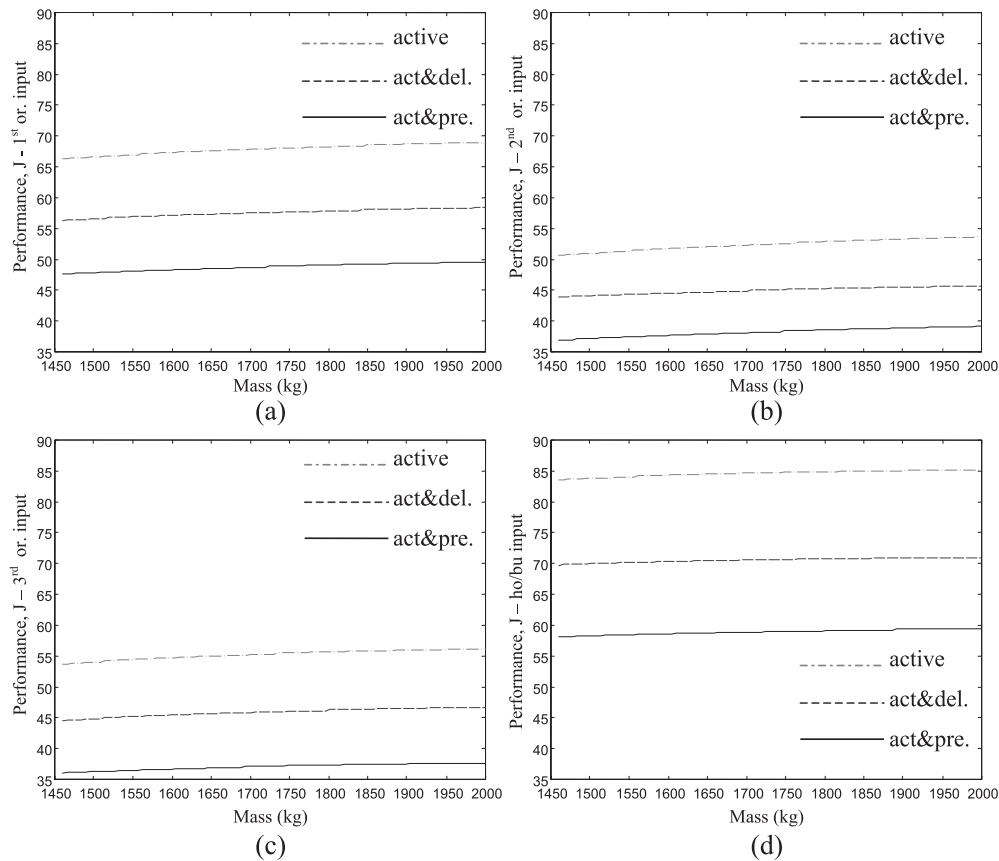


Figure 8. Variations of the normalized performance index vehicle mass for ride comfort preferences for different road excitations. (a) First order filter road input. (b) Second order filter road input. (c) Third order filter road input. (d) Hole/bump road input.

5. CONCLUSION

Performances of active, active and delay, and active and preview control systems for the suspensions of a three-dimensional car subject to random and deterministic road excitations are evaluated and the results are compared with those for the passive system. Road information from further ahead is used as the preview and the time delay between the front and the rear wheels are included in the optimal control analysis. Attention was also given to the vehicle roll acceleration by the unsymmetrical road excitations. Performance index is optimized in both ride comfort and ride holding preference. On the basis of the results presented, the following conclusion are drawn:

1. Properly designed optimal active control suspensions are highly effective in improving performance index and the vehicle mean-square acceleration responses under rough road excitations.

2. The acceleration response for optimal preview control are much lower in ride comfort preference than road holding, while suspension space and tire deflection of road holding preference are lower than ride comfort.
3. Mean-square responses of the active control suspension systems improve from active, to active and delay, and to active and preview, respectively.
4. Optimal preview control shows considerable improvements of the performance index and mean square acceleration responses for all type of road excitations.
5. A rather short time preview information of the road input is sufficient for improving the performance of the control system.
6. The performance of control system improves with an increase in the preview time up to a certain value. Further increase in the preview time does not produce significant improvement.
7. Magnitude of the control power together with dissipated power by damper for active and preview control are less than active control and both are less than passive system.
8. Performance index is not sensitive to the sprung mass variations (due to variations in the number of passengers) for all types road input models.
9. Optimal preview control improves the suspension performance for all filtered white noise road irregularities.
10. Active suspension reduces all components of mean-square accelerations including vertical, pitch and roll of the sprung mass.

REFERENCES

- Bender, E. K., 1968, "Optimum linear preview control with application to vehicle suspension," *Journal of Basic Engineering*, pp. 213–221.
- Cebon, D., and Newland, E. D., 1983, "The artificial generation of road surface topography by the inverse FFT method," *Proceeding 8th IAVSD Symposium On Dynamics of Vehicles on Roads and on Railway Tracks*, Cambridge MA, pp. 29–42.
- Chalasani, R. M., 1986, "Ride performance potential of active suspension – part II: Comprehensive analysis based on a full-car model," in *Symposium on Simulation and Control of Ground Vehicles and Transportation System*, ASME AMD, 80.
- Davis, B. R., and Thompson, A. G., 1988, "Optimal linear active suspensions with integral constraint," *Vehicle System Dynamics*, **18**, 357–366.
- EL-Demerdash, S. M., and Crolla, D. A., 1996, "Effect of non-linear components on the performance of a hydro-pneumatic slow-active suspension system," *Proceeding of the Institute of Mechanical Engineering*, **210**, 23–34.
- Foag, Q., and Grubel, G., 1987, "Multi-criteria control design for preview vehicle suspension systems," *World Congress on Automatic Control*, Munich, pp. 189–195.
- Hac, A., 1992, "Optimal linear preview control of active vehicle suspension," *Vehicle System Dynamics*, **21**, 167–195.
- Hac, A., and Youn, I., 1992, "Optimal semi-active suspension with preview based on a quarter car model," *ASME Journal of Vibration and Acoustics, Stress and Reliability in Design*, **114**, 84–92.
- Hac, A., and Youn, I., 1993, "Optimal design of active and semi-active suspensions including time delays and preview," *ASME Journal of Vibration and Acoustics*, **115**, 498–508.
- Heath, A. N., 1987, "Evaluation of the isotropic road roughness assumption," *Vehicle System Dynamics*, **17**, 157–160.
- Heath, A. N., 1989, "Modeling and simulation of road roughness," *Vehicle System Dynamics*, **18**, 275–284.
- Hrovat, D., 1991, "Optimal suspension performance for 2-D vehicle models," *Journal of Sound and Vibration*, **146**, 93–110.

- Huisman, R. G. M., Veldpaus F. E., Voets H. J. M., and Kok J. J., 1993, "An optimal continuous time control strategy for active suspension with preview," *Vehicle System Dynamics*, **22**, 43–45.
- Iwata, Y., and Nakano, M., 1976, "Optimal preview control of vehicle air suspension," *Bulletin of the JSME*, **19**, 1485–1489.
- Kim, D., 1997, "Investigation of active suspension of passenger cars including vehicle system dynamics and driver inputs," Ph.D. Thesis, The University of Wisconsin-Madison, DAI, 59, No. 02B.
- Krtolica, R., and Hrovat, D., 1992, "Optimal active suspension control based on a half-car model: An analytical solution," *IEEE Transactions on Automatic Control*, **37**, 528–531.
- Mehra, R. K., Amin, J. N., Hedrick, K. J., Osorio, C., and Gopalasamy, S., 1997, "Active suspension using preview information and model predictive control," *Proceeding of the IEEE International Conference on Control Applications*, pp. 860–865.
- Marzbanrad, J. R., Hojjat, Y., Zohoor, H., and Ahmadi, G., 2001, "Stochastic optimal preview control of a vehicle suspension," *Proceeding of 5th International Mechanical Engineering Conference*, Gilan University, Iran, pp. 542–552.
- Marzbanrad, J. R., Hojjat, Y., Zohoor, H., and Nikraves, S. K., 2000, "Optimal preview control design of an active suspension based on a full car model," *Scientia Iranica*, in press.
- Nagiri, S., Doi, S., Ichi, S., and Hirawa, N., 1992, "Improvement of ride comfort by preview vehicle-suspension system," *International Congress and Exposition*, Detroit, MI.
- Pilbeam, C., and Sharp, R. S., 1996, "Performance potential and power consumption of slow-active suspension systems with preview," *Vehicle System Dynamics*, **25**, 169–183.
- Prokop, G., and Sharp, R. S., 1994, "Performance enhancement of limited bandwidth active automotive suspensions by road preview," in *Proceedings of the International Conference on Control*, **1**, 173–182.
- Rill, G., 1988, "The influence of correlated random excitation processes on dynamics of vehicles," *Proceeding 8th IA VSD-Symposium Dynamics of Vehicles on Roads and on Railway Tracks*, pp. 449–459.
- Robson, J. D., 1979, "Road surface description and vehicle response," *International Journal Vehicle Design*, **1**, 25–35.
- Rotenberg, R. W., 1972, "Vehicle Suspension," Moskou, Masinostrojenie.
- Ruf, G., 1978, "The calculation of the vibrations of a four-wheeled vehicle, induced by random road roughness of the left and right track," *Vehicle System Dynamic*, **7**, 1–23.
- Rutledge, D. C., 1990, "Models for jerk optimal vehicle suspensions," Ph.D. Thesis, University of California, DAI, 51, No. 08B.
- Sasaki, M., Kamiya, J., and Shimogo, T., 1976, "Optimal preview control of vehicle suspension," *Bulletin of the JSME*, **19**, 265–273.
- Senthil, S., and Narayanan, S., 1996, "Optimal preview control of a two-def vehicle model using stochastic optimal control theory," *Vehicle System Dynamics*, **25**, 413–430.
- Sharp, R. S., and Pilbeam, C., 1994, "On the ride comfort benefits available from road preview with slow-active car suspensions," *13th IAVSD Symposium on the Dynamics of Vehicles on Roads and on Tracks Proceeding*, **23**, 437–448.
- Thompson, A. G., Davis, B. R., and Pearce, C. E. M., 1980, "An optimal linear active suspension with finite road preview," *SAE Transaction*, paper 800520, pp. 2009–2020, Pennsylvania.
- Thompson, A. G., and Pearce, C. E. M., 1998, "Physically realisable feedback controls for a fully active preview suspension applied to a half-car model," *Vehicle System Dynamics*, **30**, 17–35.
- Tomizuka, M., 1974, "The optimal finite preview problem and its application to man-machine systems," Ph.D. Thesis, Massachusetts Institute of Technology, MA.
- Tomizuka, M., 1975, "Optimal continuous finite preview problem," *IEEE Transactions on Automatic Control*, pp. 362–365.
- Tomizuka, M., 1976, "Optimal linear preview control with application to vehicle suspension revisited," *ASME Journal of Dynamical Systems, Measurement and Control*, **98**, 309–315.
- Van der Aa, M. A. H., Muijderman, J. H. E. A., and Veldpaus, F. E., 1997, "Constrained optimal control of semi-active suspension systems with preview," *Vehicle System Dynamics*, **28**, 307–323.
- William, D. E., 1995, "Active suspension control systems: Theoretical issues and experimental results (vehicle dynamics)," Ph.D. Thesis, Florida Institute of Technology, DAI, 56, No. 12B.
- Yeh, E., and Tsao, Y. J., 1994, "Fuzzy preview control scheme of active suspension for rough road," *International Journal of Vehicle Design*, **15**, 166–180.

- Yoshimura, T., and Ananthanarayana, N., 1991, "Stochastic optimal control of vehicle suspension with preview on an irregular surface," *International Journal of Systems Science*, **22**, 1599–1611.
- Yu, F., and Crolla, D. A., 1998, "An optimal self-tuning controller for an active suspension," *Vehicle System Dynamics*, **29**, 51–66.
- Zaremba, A., Hampo, R., and Hrovat, D., 1997, "Optimal active suspension design using constrained optimization," *Journal of Sound and Vibration*, **207**, 351–365.